NORSAR Scientific Report No. 1-2013

Semiannual Technical Summary

1 January – 30 June 2013

Tormod Kværna (Ed.)

Kjeller, December 2013

6.2 Examination of the Storfjorden Aftershock Sequence Using an Autonomous Event Detection and Grouping Framework: Preliminary Results

6.2.1 Introduction

The Storfjorden aftershock sequence was triggered by a M_w 6.2 earthquake that occurred off the Svalbard archipelago's southeastern coast on February 21, 2008. Over the last five years, it has generated thousands of aftershocks; several have exceeded M_w 4.0. Fig. 6.2.1 shows the locations (in green) of sequence events published in NORSAR's analyst reviewed regional bulletin. Pirli *et al.* (2013) and Junek *et al.* (2014) conducted an investigation of the regional seismotectonics and concluded the source of the sequence was not related to the nearby Billefjorden fault zone. Instead, its source is most likely tied to the Tertiary shear zone shown in red in Fig. 6.2.1. This conclusion is supported by the orientation of the relative relocation catalog, shown in blue in Fig. 6.2.1, and the orientations of focal mechanisms for numerous sequence events (Pirli *et al.*, 2013; Junek *et. al.*, 2014).

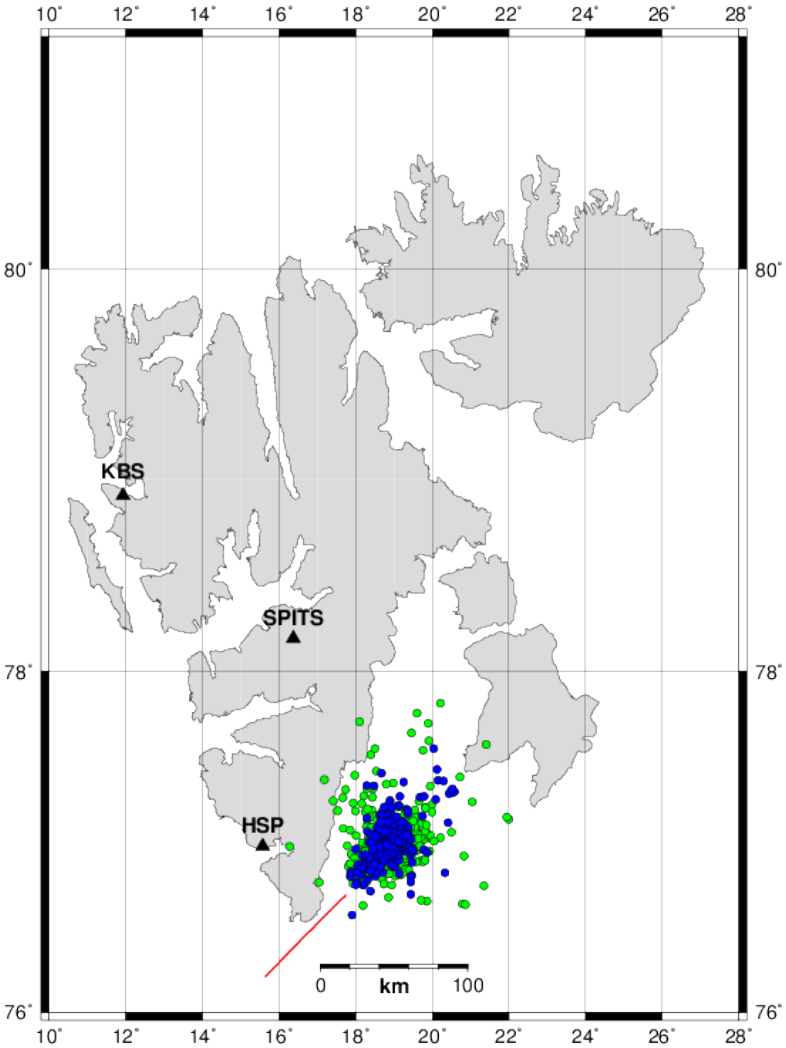

Fig. 6.2.1
The Storfjorden aftershock sequence occurred off Spitsbergen's southeast coast. Events shown in green represent the NORSAR analyst reviewed catalog between 21 February 2008 and 20 April 2012. Blue events represent the relative relocation catalog (Pirli et. al., 2013). The red line shows the location of the shear zone suggested by Bergh and Grogan (2003), believed to be related with the Storfjorden sequence (Pirli et. al., 2013). Black triangles show the locations of some of the permanent seismic stations on Spitsbergen.

The results shown in previous studies (Pirli et. *al.*, 2013; Junek et. *al.*, 2014) were largely based on the analysis of manually reviewed events. However, the number of events in the NORSAR analyst reviewed bulletin represents a small fraction of the total number of events produced by the sequence. Here, an autonomous event detection and clustering framework is used to expand the available dataset. The expanded dataset will be used in future studies to infer additional information about the tectonic structure within the fjord and to examine the sequence's spatiotemporal properties.

The detection framework is a Java based application that was developed as a collaborative effort between Lawrence Livermore National Laboratory and NORSAR. A block diagram of the framework's core functionality is shown in Fig. 6.2.2 and a complete description of an early version of the system is provided in Harris and Dodge (2011). The framework uses power (STA/LTA) detectors operating on array beams to detect events with new waveform patterns, and automatically spawns correlation detectors to search for additional occurrences of events with those patterns. The framework maintains a pool of such empirically-derived correlation detectors, which may be updated upon the detection of new signals approximately matching the patterns. It groups signal detections based on waveform similarity and stores event affiliation information in a relational database. All framework detections are tagged with an identification number (detector ID) that represents new or previously observed signal types. The database can be mined to study the various aspects of the sequence. For example, detector IDs can be grouped and associated detections counted to identify event clusters.

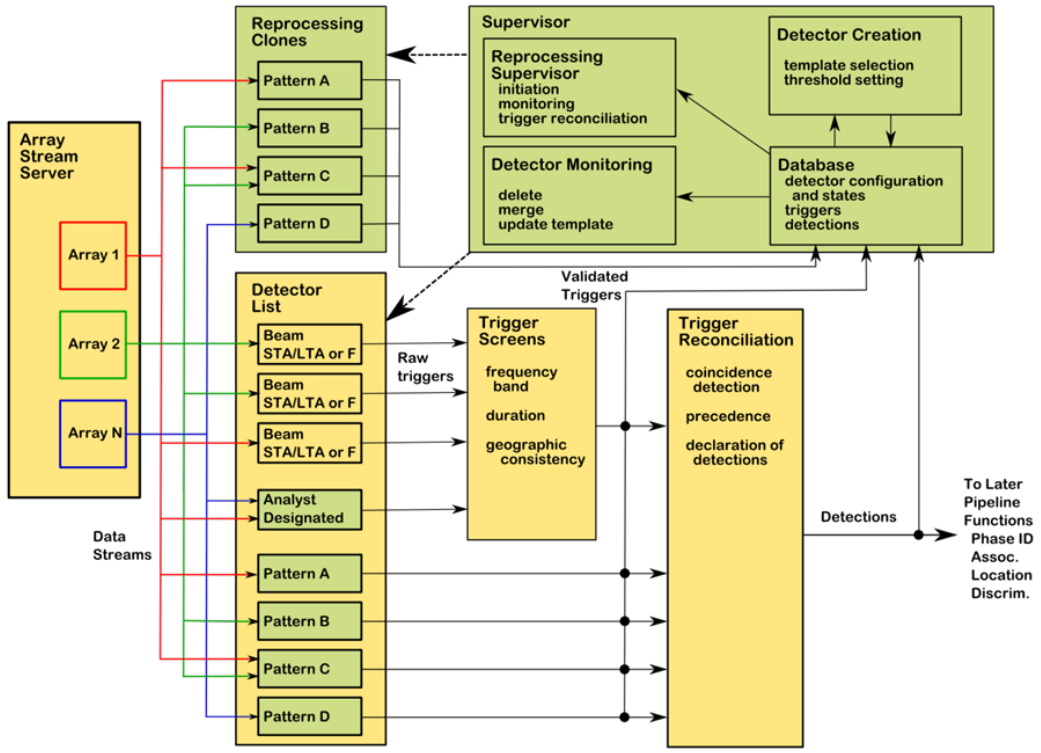

Fig. 6.2.2 Autonomous seismic event detection and grouping framework block diagram.

6.2.2 Completeness Magnitude Estimation

In this study event size is estimated using a relative magnitude (mb_{rel}) relationship that scales newly detected events against a user defined master event. The relative scaling relationship used in this study is defined as

$$mb_{rel} = mb_r + \log_{10}(A_n / A_r) \quad (1)$$

where mb_r is the reference event bodywave magnitude, A_r is the peak amplitude of the reference event seismogram, and A_n is the peak amplitude of the new event seismogram. This relation allows the reference magnitude to be adjusted as a function of the log amplitude ratio. Since all of the events under consideration originate in a small area, no distance correction is needed. The relative magnitude scale allows bodywave magnitudes to be calculated for all SPITS empirical signal detector (ESD) detections. Relative magnitude estimates are used to produce a cumulative frequency magnitude distribution (FMD) that quantifies the detection threshold for SPITS relative to the Storfjorden region.

Determination of the catalog completeness magnitude (M_c) is performed using the method outlined in Wiemer and Wyss (2000). Their method compares the linear sections of the observed and model FMD between the maximum magnitude and an assumed M_c. The goodness-of-fit (GOF) between the modeled and observed FMDs is assessed using

$$R(a,b,M_i) = 100 - \frac{\sum_{M_i}^{M_{max}} |B_i - S|}{\sum_i B_i} 100 \quad (2)$$

where R is the GOF, a and b are the Gutenberg-Richter relationship parameters, M_i is the completeness magnitude being tested, and B and S are the observed and predicted portions of the distribution for each magnitude bin. The Gutenberg-Richter coefficients are determined via least-squares regression before the initiation of the M_c estimation routine. This is an iterative process that tests the validity of many M_c values. Here, the M_c value with the largest GOF measurement is chosen as the catalog completeness magnitude.

6.2.3 Results

The detection framework was used to process waveform data from 7 vertical, broadband, elements of the SPITS array between 21 February 2008 and 20 April 2012. Processing parameter values and descriptions for the four year processing run are listed in Table 6.2.1. The array power detector threshold was set high so only high-quality signals were used as ESD templates. Since our ESDs have a large time bandwidth product and use multiple channels of the array, the correlation detector threshold, T_{ESD}, was set to 0.2. Frequency-Wavenumber (FK) screening was used to remove detections originating outside of Storfjorden. Signal duration was used as an additional screening metric. Valid detections had durations that fell between TL_{min} and TL_{max}.

Table 6.2.1. Processing parameters employed by detection framework for Storfjorden sequence for SPITS array.

Parameter	Value	Description
Filter Type	Bandpass	3 Pole, Butterworth
F_{lo}	2.0 Hz	Filter Low Frequency Coner
F_{hi}	8.0 Hz	Filter High Frequency Corner
TL_{min}	20.0 sec	Minimum Template Length
TL_{max}	33.0 sec	Maximum Template Length
Azimuth	150.0 deg	Detection Beam Azimuth
Velocity	6.2 km/sec	Detection Beam Velocity
Az_{tol}	+/- 20.0 deg	Azimuth Tolerance
Vel_{tol}	+/- 1.0 km/sec	Velocity Tolerance
T_{AP}	20.0	Array Power Detection Threshold
T_{EDS}	0.2	ESD Threshold
FK_{pow}	0.3	Minimum FK Power

Table 6.2.2. Detection framework results, where Y denotes the application of FK screening and N its absence.

Parameter	FK Screening	Results
Detections	Y	15911
	N	76688

The total number of detections and event clusters produced by the detection framework are listed in Table 6.2.2. FK screening was invoked during post processing via an application that runs outside the detection framework. As a result, all array power detections were used to spawn new correlation detectors regardless of their slowness vector. Since the SPITS array observes seismicity from numerous local, regional, and teleseismic sources, a large number of detectors were formed from sources outside of Storfjorden.

Figs. 6.2.3 and 6.2.4 show FK measurements for all detections made over the four-year processing interval. Black dots indicate events that fell within the azimuth, velocity, and FK power constraints listed in Table 6.2.1 and red dots indicate those events which did not. The time series plot shows detections were typically made along the 60, 150, 220, and 330 degree azimuths. The polar plot shows numerous sources of repeating seismicity near the station. Repeating sources include, mining activity, ice quakes, local earthquakes, Mid-Atlantic Ridge earthquakes, and Storfjorden events (shown in black). The large number of off-target detections highlights the need for post detection azimuth and slowness screening for the automatically generated ESDs. Approximately 80% of the detections were rejected after the screening metrics were applied.

Figs. 6.2.5 and 6.2.6 show the magnitude distributions and M_c estimates for the framework and NORSAR catalogs. FMDs have similar b-values and highlight detection threshold differences between the two catalogs. M_c estimates for the framework and NORSAR catalogs with the largest GOF values are 0.8 and 2.1. The difference in M_c estimates shows the framework is providing a 1.3 magnitude unit improvement in detection capability for Storfjorden events observed by SPITS.

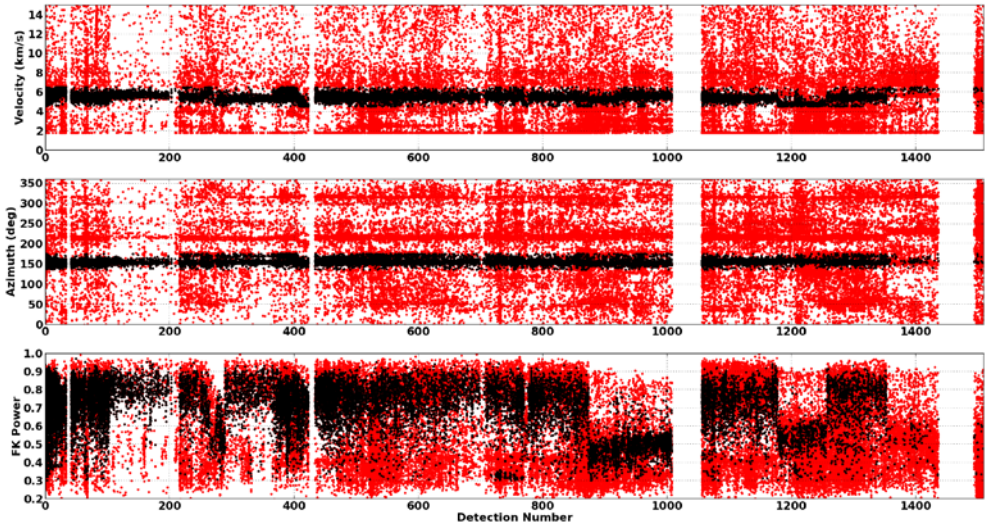

Fig. 6.2.3 FK measurements for framework detections, where the top plot is velocity, center is back azimuth, bottom is FK power, red dots represent all detections, and black dots denotes detections that passed the screening criteria. The numbers on the x-axis denote the number of days after the start of the sequence (21 February 2008). Gaps in data availability are observed near days 5, 410, 1010, and 1450.

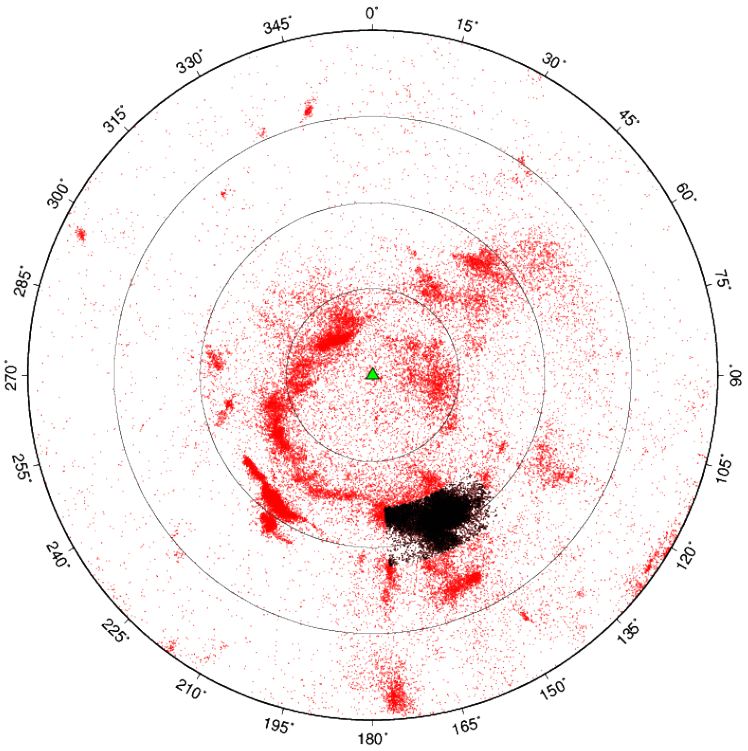

Fig. 6.2.4 Azimuth (angle axis) and slowness measurements (radius axis), where the distance between concentric circles is 0.1 sec/km. The green triangle denotes the SPITS array.

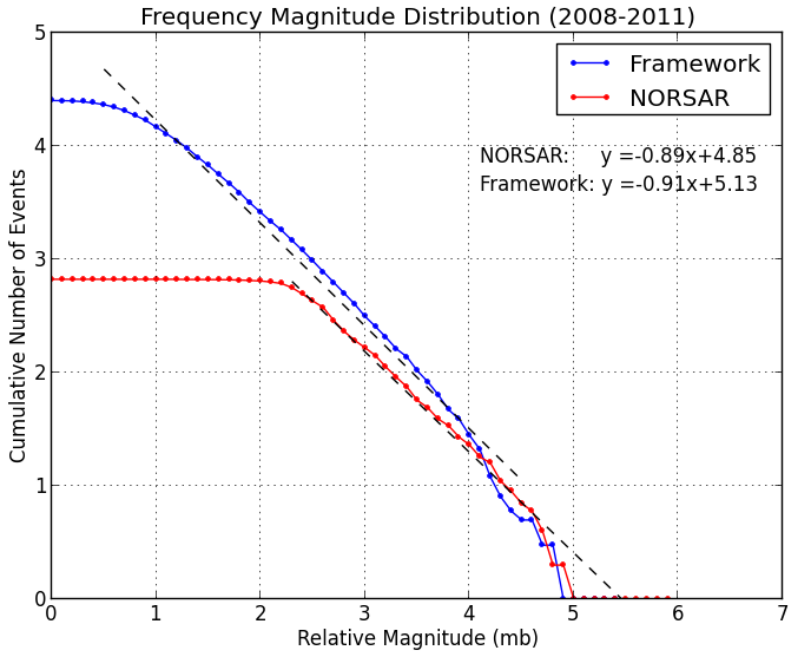

Fig.6.2.5 Cumulative FMD for framework (blue) and NORSAR (red) catalogs.

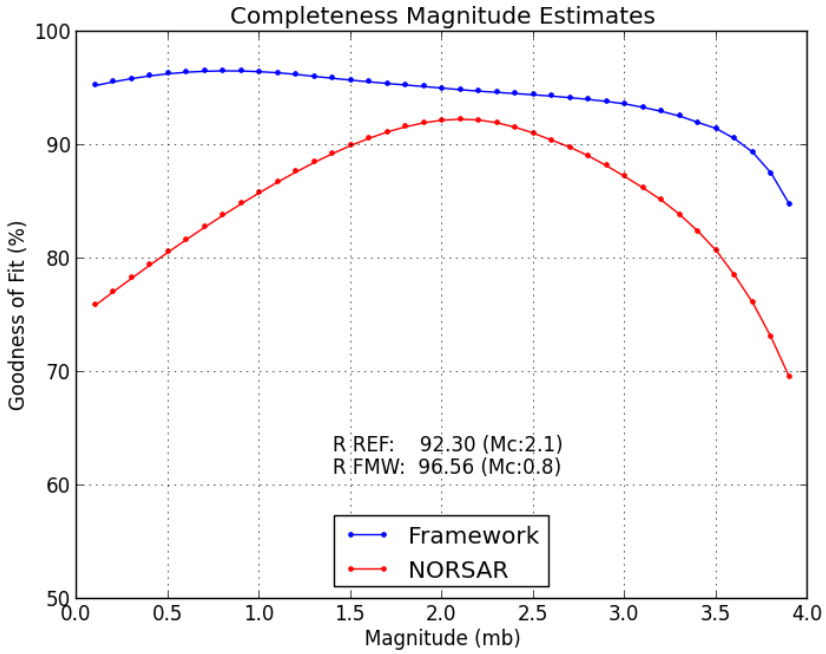

Fig. 6.2.6 GOF measurements for the linear portion of the modeled and observed frequency magnitude distributions for the framework (blue) and NORSAR (red) catalogs.

The initiation day, lifespan, and number of events in each cluster are shown in Fig. 6.2.7. Lifespan bars show the onset and duration of each cluster. The cluster generation rate is greatest at the beginning of the sequence and remains relatively constant until day 100. At this point, the rate decreases and spikes on days where reactivation episodes occur. The lifespan of the clusters vary dramatically, where some last hours and others live for the entire length of the sequence. The

number of events constituting each cluster also varies significantly. Some groups have a single member, while others have between 10 and 85 members.

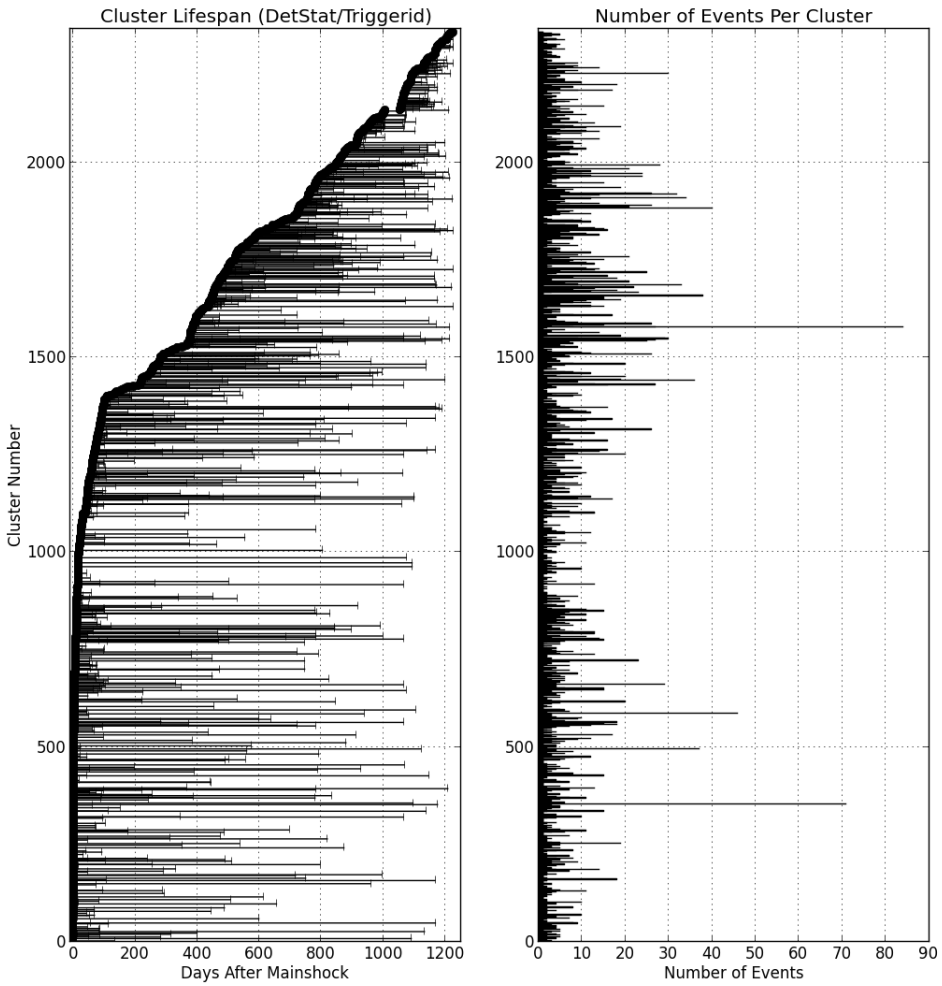

Fig. 6.2.7 Cluster lifespan (left panel) and number of events per cluster (right panel), where each point on the lifespan bars represents the initiation time of the cluster.

6.2.4 Summary

We have demonstrated the use of an autonomous event detection and grouping system for studying the 2008 Storfjorden aftershock sequence. The system exploited data from the SPITS array and produced an event catalog whose completeness is 1.3 magnitude units lower than the NORSAR analyst reviewed bulletin for Storfjorden. The cluster lifespan plot highlights the source heterogeneity within the fjord. The space-time distribution of clusters suggests the evolution of the sequence follows an epidemic type aftershock model Ogata (1988), rather than the smooth exponential decay predicted by Omori's law.

Future work will focus on the further application of the framework to 2008 Storfjorden sequence for inferring tectonic structure within the fjord. In addition, the spatiotemporal distribution of the events will be studied and their adherence to epidemic type aftershock sequence models will be examined.

W. N. Junek **(Air Force Technical Applications Center)**
T. Kværna **(NORSAR)**
M. Pirli **(NORSAR)**
D. B. Harris **(Deschutes Signal Processing)**
J. Schweitzer **(NORSAR)**
M. T. Woods **(Air Force Technical Applications Center)**

References

Bergh, S.G. and P. Grogan (2003). Tertiary structure of the Sørkapp-Hornsund region, South Spitsbergen, and implications for the offshore southern extension of the fold-thurst belt, *Norw. J. Geol*., **83**, 43-60.

Harris, D. B. and D. A. Dodge (2011). An Autonomous System for Grouping Events in a Developing Aftershock Sequence, *Bull. Seismol. Soc. Am.*, **101**, No. 2, 763-774.

Junek, W. N. Roman-Nieves, J. A., and M.T. Woods (2014). Tectonic Implications of Earthquake Mechanisms in Svalbard, *Geophys. J. Int.* (Accepted for publication)

Ogata, Y. (1988). Statistical Models of Earthquake Occurrences and Residual Analysis of Point Processes, *Journal of the American Statistical Association*, **83** (401), 9-27.

Pirli, M., Schweitzer, J. and B. Paulsen (2013). The Storfjorden, Svalbard, 2008-2012 Aftershock Sequence: Seismotectonics in a Polar Environment, *Tectonophysics*, **601**, 192-205.

Wiemer, S. and M. Wyss (2000). Minimum Magnitude of Completeness in Earthquake Catalogs: Examples from Alaska, The Western United States, and Japan, *Bull. Seismol. Soc. Am.*, **90**, No. 4, 859-869.